Inorg. Chem. **2001,** *40,* 1459−1465

Syntheses of Ru−S Clusters with Kinetically Labile Ligands via the Photolysis of $[(\text{cymene})_3Ru_3S_2](PF_6)_2$

Amanda L. Eckermann,[†] Dieter Fenske,[‡] and Thomas B. Rauchfuss*[,†]

School of Chemical Sciences, University of Illinois, Urbana, Illinois, and Lehrstuhl für Anorganische Chemie, Technische Universität Karlsruhe, Karlsruhe, Germany

Received September 19, 2000

Three ruthenium sulfide clusters with labile CH_3CN ligands have been photochemically synthesized. Irradiation of $[(\text{cymene})_3Ru_3S_2](PF_6)_2$ ([**1**]$(PF_6)_2$) in CH_3CN gives $[(\text{cymene})_2(CH_3CN)_3Ru_3S_2](PF_6)_2$ ([**2**]$(PF_6)_2$), which has been characterized by ^1H NMR spectroscopy, ESI mass spectrometry, and chemical reactivity. Treatment of [**2**]$(PF_6)_2$ with PPh_3 gives $[(\text{cymene})_2(CH_3CN)_2(PPh_3)Ru_3S_2](PF_6)_2$ ([**3**]$(PF_6)_2$) and $[(\text{cymene})_2(CH_3CN)(PPh_3)_2Ru_3S_2](PF_6)_2$ ([**4**]$(PF_6)_2$), while treatment with 1,4,7-trithiacyclononane (9S3) gives $[(\text{cymene})_2(9S3)Ru_3S_2](PF_6)_2$ ([**5**]$(PF_6)_2$). A crystallographic study demonstrated that the Ru_3 core in [**3**]$(PF_6)_2$, [**4**]$(PF_6)_2$, and [**5**]$(PF_6)_2$ is distorted with a pair of elongated Ru−Ru bonds. Cyclic voltammetry shows that [**3**]$(PF_6)_2$ and [**4**]$(PF_6)_2$ undergo two closely spaced reversible one-electron reductions whereas [**5**]$(PF_6)_2$ undergoes one irreversible one-electron reduction and one reversible one-electron reduction. Prolonged irradiation of [**1**]$(PF_6)_2$ in CH_3CN causes decomposition, resulting in the pentanuclear cluster $[(\text{cymene})_4Ru_5S_4](PF_6)_2$ ([**6**]$(PF_6)_2$).

Introduction

In recent years transition metal sulfides have been increasingly recognized as key industrial[1,2] and biological[3−5] catalysts. The hydrodesulfurization (HDS) process in industry uses a molybdenum−cobalt−sulfide (Mo/Co/S) catalyst although other metal sulfides (e.g., RuS_2) are superior.[6,7] In nature, metal sulfido clusters are essential components in many fundamental processes such as electron transfer, reduction of dinitrogen, and reactions involving CO.[8−10] One important characteristic of these metal sulfido catalysts is the presence of kinetically accessible coordination sites, i.e., the presence of coordinative unsaturation or the kinetic labile of ligands.

In general, we are interested in the design of metal sulfide catalysts inspired by precedents in biology. A prime example of a catalyst for reducing small, unsaturated (π-acceptor) molecules under mild conditions is nitrogenase.[11] The active site features an electroactive Fe−Mo−S cluster[12] with low-coordinate iron sulfido centers.[13] With nitrogenase as a model, related *cluster-based* catalysts should exhibit the following specific features: (1) coordinatively unsaturated or kinetically labile metal sites to provide a binding site for substrates, (2) low-valent (0 to 2+) or electron-rich metals to encourage binding of electrophilic substrates, (3) redox activity to facilitate heterolytic activation of H_2, and (4) kinetically or thermodynamically stable cluster core. Sulfur ligation per se is not crucial to these requirements, but it does provide a convenient and proven means of strongly linking metal atoms, pertinent to item 4. Perhaps the most difficult aspect of the above criteria is the concomitant need for cluster stability and kinetically accessible coordination sites.

Previously synthesized ruthenium sulfide compounds exhibit some, but not all, of these features. For example, virtually all known ruthenium sulfido clusters are kinetically inert. The CO- and Cp-containing species are notoriously sluggish to undergo ligand exchange. The species $(MeC_5H_4)_4Ru_4S_4$ is redox-active but coordinatively saturated.[14−16] The trinuclear cluster $[(\text{cymene})_3Ru_3S_2](PF_6)_2$ is redox-active, features low-valent metals, and has a robust Ru_3S_2 core (criteria 2−4);[17] however, the cymene ligands block the metal sites. While such inertness conferred by the cymene ligands facilitates structural and mechanistic studies, the cymene ligands would need to be removed in order to allow for cluster-based catalysis. In this paper we address this problem.

It is well-known that η^6-arene ligands on Ru(II) species can be labilized. Heat or ultraviolet irradiation triggers arene exchange in the compounds $(\text{arene})RuCl_2PR_3$ (arene = benzene,

---

[†] University of Illinois.

[‡] Technische Universität Karlsruhe.

(1) Pecoraro, T. A.; Chianelli, R. R. *J. Catal.* **1981**, *67*, 430−445.

(2) Kelty, S. P.; Li, J.; Chen, J. G.; Chianelli, R. R.; Ren, J.; Whangbo, M. H. *J. Phys. Chem. B* **1999**, *103*, 4649−4655.

(3) Kim, J.; Woo, D.; Rees, D. C. *Biochemistry* **1993**, *32*, 7104−7115.

(4) Chan, M. K.; Kim, J.; Rees, D. C. *Science* **1993**, *260*, 792−794.

(5) Lloyd, S. J.; Lauble, H.; Prasad, G. S.; Stout, C. D. *Protein Sci.* **1999**, *8*, 2655−2662.

(6) Topsøe, H.; Clausen, B. S.; Massoth, F. E. *Hydrotreating Catalysis, Science and Technology*; Springer-Verlag: Berlin, 1996.

(7) Tan, A.; Harris, S. *Inorg. Chem.* **1998**, *37*, 2215−2222.

(8) Armstrong, F. A. *Adv. Inorg. Chem.* **1992**, *38*, 117−163.

(9) Kaim, W.; Schwederski, B. In *Bioinorganic Chemistry: Inorganic Elements in the Chemistry of Life*; J. Wiley: Chichester, 1991; pp 128−149.

(10) Heo, J. Y.; Staples, C. R.; Halbleib, C. M.; Ludden, P. W. *Biochemistry* **2000**, *39*, 7956−7963.

(11) Burgess, B. K.; Lowe, D. J. *Chem. Rev.* **1996**, *96*, 2983−3011.

(12) Smith, B. E.; Durrant, M. C.; Fairhurst, S. A.; Gormal, C. A.; Gronberg, K. L. C.; Henderson, R. A.; Ibrahim, S. K.; Le Gall, T.; Pickett, C. J. *Coord. Chem. Rev.* **1999**, *186*, 669−687.

(13) Peters, J. W.; Stowell, M. H. B.; Soltis, S. M.; Finnegan, M. G.; Johnson, M. K.; Rees, D. C. *Biochemistry* **1997**, *36*, 1181−1187.

(14) Houser, E. J.; Amarasekera, J.; Rauchfuss, T. B.; Wilson, S. R. *J. Am. Chem. Soc.* **1991**, *113*, 7440−7442.

(15) Houser, E. J.; Rauchfuss, T. B.; Wilson, S. R. *Inorg. Chem.* **1993**, *32*, 4069−4076.

(16) Houser, E. J.; Venturelli, A.; Rauchfuss, T. B.; Wilson, S. R. *Inorg. Chem.* **1995**, *34*, 6402−6408.

(17) Lockemeyer, J. R.; Rauchfuss, T. B.; Rheingold, A. L. *J. Am. Chem. Soc.* **1989**, *111*, 5733−5738.

10.1021/ic0010609 CCC: \$20.00

toluene, *p*-cymene, etc.).[18] Upon exposure to intense UV radiation, solutions of $(C_5R_5)Ru(arene)^+$ (R = H, Me) in acetonitrile give $(C_5R_5)Ru(CH_3CN)_3{}^+$,[19] which has been used as a source of the $(C_5R_5)Ru^+$ unit in the synthesis of a wide variety of complexes.[20−22] Arene ligands can also be replaced by H_2O in the photoaquation of $(arene)Ru(NH_3)_3{}^{2+}$ and $(arene)Ru(H_2O)_3{}^{2+}$ to give $Ru(H_2O)_3(NH_3)_3{}^{2+}$ and $Ru(H_2O)_6{}^{2+}$, respectively.[23] Related photolytic routes have been used to produce $(arene)Ru(CH_3CN)_3{}^{2+}$ and $Ru(CH_3CN)_6{}^{2+}$ from sandwich compounds.[24] Both $Ru(H_2O)_6{}^{2+}$ and $Ru(CH_3CN)_6{}^{2+}$ are active polymerization catalysts for strained olefins.[25] In view of this prior work, we recognized that the trinuclear cluster $[(cymene)_3Ru_3S_2](PF_6)_2$ is a promising candidate for modification by photolytic removal of one or more of its arene ligands.

Results

$[(cymene)_2(CH_3CN)_3Ru_3S_2](PF_6)_2$ ([2](PF_6)$_2$). ^1H NMR spectroscopic analysis revealed that photolyses of CD_3CN solutions of [**1**]$(PF_6)_2$ resulted in the concomitant formation of both free cymene and a new cymene-containing species ([**2**-d_9]$(PF_6)_2$). Complete conversion of [**1**]$(PF_6)_2$ to [**2**-d_9]$(PF_6)_2$ occurred in ca. 2 h for 2 mM solutions:

$$\underset{\mathbf{1}}{[(cymene)_3Ru_3S_2]^{2+}} \xrightarrow[CD_3CN]{h\nu} \underset{\mathbf{2}\text{-}d_9}{[(cymene)_2(CD_3CN)_3Ru_3S_2]^{2+}} + \text{cymene} \quad (1)$$

Arene displacement does not occur thermally; labilization of cymene ligands was determined to be a purely photochemical process. Samples of [**1**]$(PF_6)_2$ in CD_3CN exhibited no free cymene after being refluxed in darkness for 4 h. Room light (fluorescent) and sunlight, however, did convert [**1**]$(PF_6)_2$ to [**2**]$(PF_6)_2$ over the course of days. Extended exposure of CH_3CN solutions of [**1**]$(PF_6)_2$ to UV light, sunlight, or room light resulted in decomposition.

On the basis of the NMR integration of the photolysis products, [**2**-d_9]$(PF_6)_2$ has the formula $[(cymene)_2(CD_3CN)_xRu_3S_2](PF_6)_2$, and we assume $x = 3$ based on electron counting rules as well as subsequent experiments. ESI-MS of a photolysis solution revealed a peak at $m/z = 339$ corresponding to $[(cymene)_2(CD_3CN)Ru_3S_2]^{2+}$ as well as weaker peaks at $m/z = 362$ and 384 for $[(cymene)_2(CD_3CN)_2Ru_3S_2]^{2+}$ and $[(cymene)_2(CD_3CN)_3Ru_3S_2]^{2+}$, respectively. The ^1H NMR signals for the aromatic protons on the cymene ligands in [**2**-d_9]$(PF_6)_2$ are shifted by ca. 0.1 ppm upfield with respect to compound [**1**]$(PF_6)_2$. Also, the appearance (separations between peaks) of the AA′BB′ quartet is different from that of [**1**]$(PF_6)_2$, consistent with lowered symmetry. Signals for the other groups are shifted more subtly.

The photolysis of [**1**]$(PF_6)_2$ in solvents other than CH_3CN was also examined, although with limited success. Photolysis of [**1**]$(PF_6)_2$ in acetone, water, or benzonitrile resulted in no reaction. The photolysis of [**1**]Cl_2 in H_2O also yielded only starting material. Photolysis of solutions containing small amounts of CH_3CN in acetone or THF did, however, produce [**2**]$(PF_6)_2$, although more slowly than in pure CH_3CN.

Attempts to isolate $[(cymene)_2(CH_3CN)_3Ru_3S_2](PF_6)_2$ were unsuccessful. Elemental analyses of isolated samples always deviated from the calculated values by several percent. Recrystallization from CH_3CN and ether did not improve the analyses. Mass spectrometry of this recrystallized material indicated the presence of a mixture of cationic compounds including what appears to be the main decomposition product $[(cymene)_4Ru_5S_4]^{2+}$ ([**6**]$(PF_6)_2$), which is described below. Exposure of [**2**]$(PF_6)_2$ to CH_2Cl_2 resulted in significant decomposition.

Derivatives of $[(cymene)_2(CH_3CN)_3Ru_3S_2](PF_6)_2$. To support the proposed formation of [**2**]$(PF_6)_2$, we explored the syntheses of stable derivatives. ^1H NMR spectroscopy indicated that treatment of a freshly prepared CD_3CN solution of [**2**]$(PF_6)_2$ with an excess of PPh_3 gave a single new cymene-containing product. From preparative-scale reactions, we obtained good yields of the salt $[(cymene)_2(CH_3CN)_2(PPh_3)Ru_3S_2](PF_6)_2$ ([**3**]$(PF_6)_2$) as brown microcrystals. The ^1H NMR spectrum of [**3**]$(PF_6)_2$ indicated equivalent cymene ligands and the presence of one PPh_3 ligand. A signal for bound CH_3CN was not observed in a CD_3CN solution of [**3**]$(PF_6)_2$; instead, a peak for free CH_3CN (δ 1.96) was observed, indicating that the CH_3CN ligands in [**3**]$(PF_6)_2$ are kinetically labile. In the noncoordinating solvents acetone-d_6 and CD_2Cl_2, a singlet for the bound CH_3CN ligands was observed at δ 2.38 and 2.41, respectively. The ^{31}P NMR spectrum for [**3**]$(PF_6)_2$ consists of a signal at δ 67.1 as well as a septet at δ −143 for the $PF_6{}^-$. ESI-MS measurements also indicate that the acetonitrile ligands in [**3**]$(PF_6)_2$ are labile:

$$\underset{\mathbf{3}}{[(cymene)_2(CH_3CN)_2(PPh_3)Ru_3S_2]^{2+}} \underset{CH_3CN}{\overset{CD_3CN}{\rightleftharpoons}} \underset{\mathbf{3}\text{-}d_6}{[(cymene)_2(CD_3CN)_2(PPh_3)Ru_3S_2]^{2+}} \quad (2)$$

The ESI-MS analysis of a THF solution of [**3**]$(PF_6)_2$ shows peaks for $[(cymene)_2(PPh_3)Ru_3S_2]^{2+}$ as well as weaker peaks for $[(cymene)_2(CH_3CN)_2(PPh_3)Ru_3S_2]^{2+}$ and $[(cymene)_2(CH_3CN)(PPh_3)Ru_3S_2]^{2+}$, whereas a measurement of a CH_3CN solution gave a similar mass spectrum, but the signal for $[(cymene)_2(PPh_3)(CH_3CN)Ru_3S_2]^{2+}$ was the most intense.

The structure of [**3**]$(PF_6)_2$ was established by crystallographic analysis (Figure 1, Table 1). Like **1**, the cation features the familiar trigonal bipyramidal *closo*-Ru_3S_2 core, with two intact η^6-cymene ligands.[17] The average Ru−Ru distance is 2.810 Å, 0.056 Å longer than in **1** (Figure 5) but consistent with Ru−Ru bonding. The Ru_3 triangle core is distorted from D_{3h} symmetry to C_{2v} because the Ru−Ru bonds between the (cymene)Ru and $(CH_3CN)_2PPh_3Ru$ vertexes are longer (2.850 and 2.817 Å) than the Ru−Ru bond between the two (cymene)Ru vertexes (2.762 Å). The average Ru−S distance of 2.276 Å does not differ significantly from Ru−S single bonds in other μ_3-S−Ru_3 clusters and is similar to that reported for **1** (2.267 Å).[26,27] An analogue of [**3**]$(PF_6)_2$ is $Cp^*{}_2(CO)_2(PPh_3)Ru_3S_2$, formed by carbonylation of $Cp^*{}_2(H)_2(PPh_3)_2Ru_3S_2$.[28] Each adopts a closo structure consistent with a 48-electron count.

---

(18) Bennett, M. A.; Smith, A. K. *J. Chem. Soc., Dalton Trans.* **1974**, 233−241.

(19) Gill, T. P.; Mann, K. R. *Organometallics* **1982**, *1*, 485−488.

(20) McNair, A. M.; Boyd, D. C.; Bohling, D. A.; Gill, T. P.; Mann, K. R. *Inorg. Chem.* **1987**, *26*, 1182−1185.

(21) Koefod, R. S.; Mann, K. R. *Inorg. Chem.* **1989**, *28*, 2285−2290.

(22) McNair, A. M.; Boyd, D. C.; Mann, K. R. *Organometallics* **1986**, *5*, 303−310.

(23) Weber, W.; Ford, P. C. *Inorg. Chem.* **1986**, *25*, 1088−1092.

(24) Karlen, T.; Hauser, A.; Ludi, A. *Inorg. Chem.* **1994**, *33*, 2213−2218.

(25) Karlen, T.; Ludi, A.; Muhlebach, A.; Bernhard, P.; Pharisa, C. *J. Polym. Sci., Part A: Polym. Chem.* **1995**, 1665−1674.

(26) Mizobe, Y.; Hashizume, K.; Murai, T.; Hidai, M. *Chem. Commun.* **1994**, 1051−1052.

(27) Hashizume, K.; Mizobe, Y.; Hidai, M. *Organometallics* **1995**, *14*, 5367−5376.

(28) Kuwata, S.; Andou, M.; Hashizume, K.; Mizobe, Y.; Hidai, M. *Organometallics* **1998**, *17*, 3429−3436.

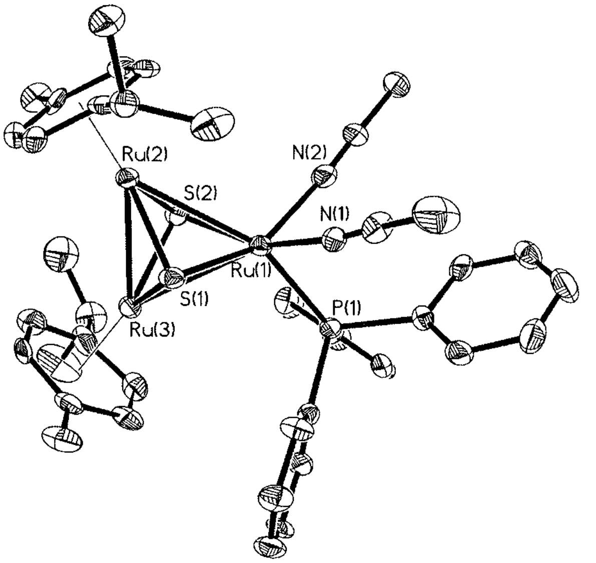

Figure 1. Thermal ellipsoid plot of **3**, $[(cymene)_2(MeCN)_2(PPh_3)Ru_3S_2]^{2+}$, drawn at 35% probability level.

Table 1. Selected Bond Lengths [Å] and Angles [deg] for the Two Molecules in the Asymmetric Unit of Compound **3**, $[(cymene)_2(MeCN)_2(PPh_3)Ru_3S_2](PF_6)_2$

	Molecule 1		
Ru(1)−Ru(2)	2.8506(16)	Ru(2)−Ru(1)−Ru(3)	58.33(3)
Ru(1)−Ru(3)	2.8175(15)	Ru(1)−Ru(2)−Ru(3)	60.24(4)
Ru(2)−Ru(3)	2.7623(16)	Ru(1)−Ru(3)−Ru(2)	61.43(4)
Ru(1)−N(1)	2.082(13)	N(1)−Ru(1)−N(2)	85.8(4)
Ru(1)−N(2)	2.077(9)	N(1)−Ru(1)−P(1)	87.5(3)
Ru(1)−P(1)	2.293(3)	N(2)−Ru(1)−P(1)	89.7(3)
Ru(1)−S(1)	2.271(3)	S(1)−Ru(1)−S(2)	89.24(11)
Ru(1)−S(2)	2.272(3)		
Ru(2)−S(1)	2.301(3)		
Ru(2)−S(2)	2.277(3)		
Ru(3)−S(1)	2.263(3)		
Ru(3)−S(2)	2.272(3)		
	Molecule 2		
Ru(4)−Ru(5)	2.8498(17)	Ru(5)−Ru(4)−Ru(6)	58.21(4)
Ru(4)−Ru(6)	2.8274(16)	Ru(4)−Ru(5)−Ru(6)	60.49(4)
Ru(5)−Ru(6)	2.7614(15)	Ru(4)−Ru(6)−Ru(5)	61.30(4)
Ru(4)−N(3)	2.076(12)	N(3)−Ru(4)−N(4)	83.9(5)
Ru(4)−N(4)	2.095(11)	N(3)−Ru(4)−P(2)	86.3(3)
Ru(4)−P(2)	2.296(3)	N(4)−Ru(4)−P(2)	91.1(3)
Ru(4)−S(3)	2.264(3)	S(3)−Ru(4)−S(4)	89.33(11)
Ru(4)−S(4)	2.264(3)		
Ru(5)−S(3)	2.289(3)		
Ru(5)−S(4)	2.289(3)		
Ru(6)−S(3)	2.267(3)		
Ru(6)−S(4)	2.272(3)		

The conversion of CH_3CN solutions of [**2**]$(PF_6)_2$ to a bis(PPh_3) derivative was very slow. However, the derivative $[(cymene)_2(CH_3CN)(PPh_3)_2Ru_3S_2](PF_6)_2$ was eventually isolated by using the more weakly coordinating solvent acetone and a large excess of PPh_3. The structure of [**4**]$(PF_6)_2$ was also established by crystallographic analysis (Figure 2, Table 2). Again, the Ru-containing cluster may be described as a trigonal bipyramidal *closo*-Ru_3S_2 core, with two η^6-cymene ligands. Relative to [**3**]$(PF_6)_2$, the Ru_3 triangle core in [**4**]$(PF_6)_2$ is further distorted from D_{3h} symmetry with an average Ru−Ru distance of 2.850 Å. The two longer Ru−Ru distances are 2.861 and 2.949 Å, vs 2.77 and 2.81 Å in [**1**]$(PF_6)_2$ and [**3**]$(PF_6)_2$, respectively, but are still interpreted as bonding (Figure 5). The distortion of the Ru_3 triangle is attributed to the steric demands of the seven-coordinate $Ru(PPh_3)_2(CH_3CN)$ center. The average Ru−S distance (2.274 Å) is comparable to that of [**3**]$(PF_6)_2$ and thus also does not differ significantly from [**1**]$(PF_6)_2$.

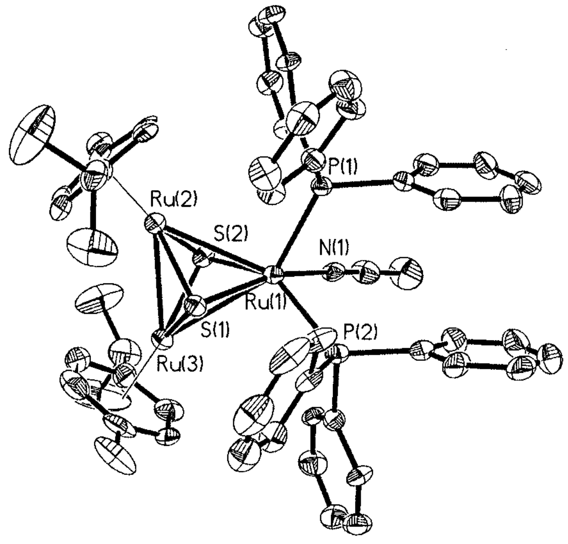

Figure 2. Thermal ellipsoid plot of **4**, $[(cymene)_2(MeCN)(PPh_3)_2Ru_3S_2]^{2+}$, drawn at 35% probability level. Hydrogen atoms are omitted for clarity.

Table 2. Selected Bond Lengths [Å] and Angles [deg] for Compound **4**, $[(cymene)_2(MeCN)(PPh_3)_2Ru_3S_2](PF_6)_2$

Ru(1)−Ru(2)	2.8604(19)	Ru(2)−Ru(1)−Ru(3)	56.26(5)
Ru(1)−Ru(3)	2.9488(15)	Ru(3)−Ru(2)−Ru(1)	63.50(5)
Ru(2)−Ru(3)	2.740(2)	Ru(2)−Ru(3)−Ru(1)	60.24(4)
Ru(1)−N(1)	2.078(7)	N(1)−Ru(1)−P(1)	86.54(18)
Ru(1)−P(1)	2.317(2)	N(1)−Ru(1)−P(2)	87.5(2)
Ru(1)−P(2)	2.412(3)	P(1)−Ru(1)−P(2)	101.09(9)
Ru(1)−S(1)	2.276(2)	S(1)−Ru(1)−S(2)	86.87(8)
Ru(2)−S(1)	2.272(3)		
Ru(3)−S(1)	2.275(2)		
Ru(1)−S(2)	2.290(2)		
Ru(2)−S(2)	2.264(3)		
Ru(3)−S(2)	2.274(2)		

Because all three CH_3CN ligands in [**2**]$(PF_6)_2$ are labile, it seemed possible to make a derivative with a tridentate ligand. Thus, a CH_3CN solution of [**2**]$(PF_6)_2$ was treated with 1,4,7-trithiacyclononane (hereafter referred to as 9S3) to give a brown powder, which was purified by recrystallization from CH_2Cl_2 and ether. Also, photolysis of a solution of [**1**]$(PF_6)_2$ and 9S3 in CD_3CN resulted in [**5**]$(PF_6)_2$ and free cymene:

$$\underset{\mathbf{1}}{[(\text{cymene})_3\text{Ru}_3\text{S}_2]^{2+}} + 9\text{S}3 \xrightarrow[\text{CD}_3\text{CN}]{h\nu} \underset{\mathbf{5}}{[(\text{cymene})_2(9\text{S}3)\text{Ru}_2\text{S}_2]^{2+}} + \text{cymene} \quad (3)$$

The ^1H NMR spectrum confirmed the ratio of two cymene ligands per one 9S3 ligand, whose signals appeared as a complex multiplet at δ 2.51. X-ray crystallography was used to resolve the structure of [**5**]$(PF_6)_2$ (Figure 3, Table 3). The average Ru−Ru distance of 2.795 Å is shorter than that for [**3**]$(PF_6)_2$ or [**4**]$(PF_6)_2$ but still significantly larger than that for [**1**]$(PF_6)_2$. The two longest Ru−Ru distances (2.829 and 2.795 Å) are within Ru−Ru bond distance limits. The average Ru−S distance (2.274 Å) is identical to that found in [**4**]$(PF_6)_2$. Overall, the structure is more comparable to that of [**3**]$(PF_6)_2$ than of [**4**]$(PF_6)_2$ (Figure 5). Ruthenium carbonyl clusters with 9S3 ligands have been reported. [29,30]

---

(29) Adams, R. D.; Falloon, S. B.; McBride, K. T.; Yamamoto, J. H. *Organometallics* **1995**, *14*, 1739−1747.

(30) Adams, R. D.; Yamamoto, J. H. *Organometallics* **1995**, *14*, 3704−3711.

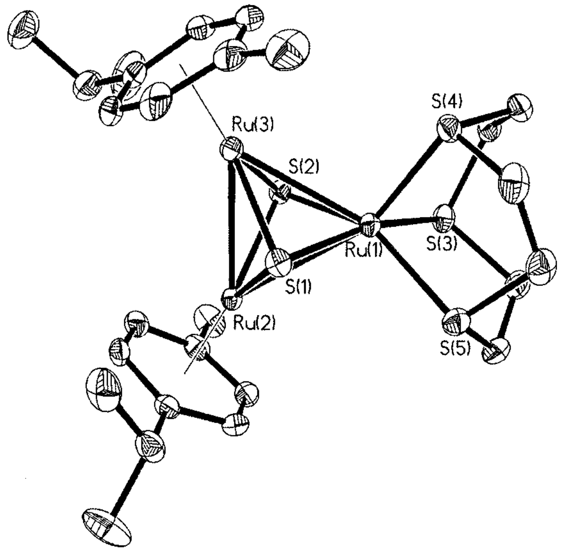

Figure 3. Thermal ellipsoid plot of **5**, $[(\text{cymene})_2(9\text{S}3)\text{Ru}_3\text{S}_2]^{2+}$, drawn at 35% probability level.

Table 3. Selected Bond Lengths [Å] and Angles [deg] for Compound **5**, $[(\text{cymene})_2(9\text{S}3)\text{Ru}_3\text{S}_2](\text{PF}_6)_2$

Ru(1)−Ru(2)	2.8287(8)	Ru(2)−Ru(1)−Ru(3)	58.83(2)
Ru(1)−Ru(3)	2.7951(10)	Ru(1)−Ru(2)−Ru(3)	59.98(2)
Ru(2)−Ru(3)	2.7621(8)	Ru(1)−Ru(3)−Ru(2)	61.19(2)
Ru(1)−S(1)	2.2763(12)	S(1)−Ru(1)−S(2)	89.73(4)
Ru(1)−S(2)	2.2663(13)	S(3)−Ru(1)−S(4)	87.25(4)
Ru(1)−S(3)	2.3586(13)	S(4)−Ru(1)−S(5)	87.82(5)
Ru(1)−S(4)	2.2854(11)	S(3)−Ru(1)−S(5)	86.78(5)
Ru(1)−S(5)	2.3310(15)		

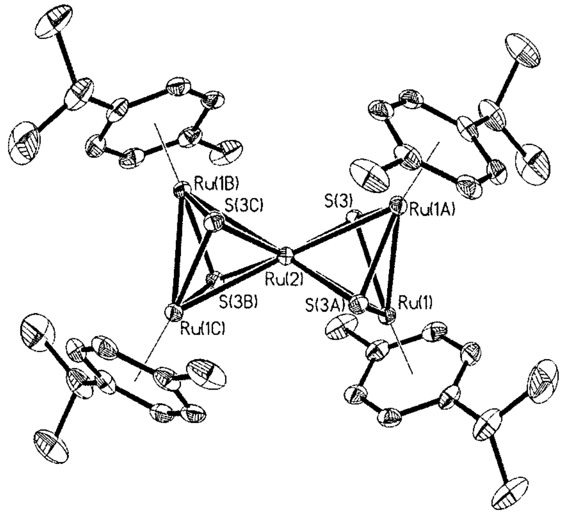

Figure 4. Thermal ellipsoid plot of **6**, $[(\text{cymene})_4\text{Ru}_5\text{S}_4]^{2+}$, drawn at 35% probability level.

Table 4. Unique Bond Lengths [Å] and Angles [deg] for Compound **6**, $[(\text{cymene})_4\text{Ru}_5\text{S}_4](\text{PF}_6)_2$[a]

Ru(1)−Ru(2)	2.7413(2)	Ru(2)−Ru(1)−Ru(1)#1	59.532(4)
Ru(1)−Ru(1)#1	2.7800(4)	Ru(1)#1−Ru(2)−Ru(1)	60.936(8)
Ru(1)−S(1)	2.2848(7)		
Ru(1)−S(1)#1	2.2825(7)		
Ru(2)−S(1)	2.2633(6)		

[a] Symmetry transformations used to generate equivalent atoms: (#1) $-y + {}^1/_4, -x + {}^1/_4, -z + {}^1/_4$; (#2) $y - {}^1/_4, x + {}^1/_4, -z + {}^1/_4$; (#3) $-x + 0, -y + {}^1/_2, z + 0$; (#4) $-x + {}^1/_2, y, -z$.

Attempted Synthesis of $[\text{Ru}_3\text{S}_2\text{L}_9]^{2+}$. Prolonged irradiation of CD_3CN solutions of [**1**]$(\text{PF}_6)_2$ for 6−12 h resulted in ratios of free cymene to bound cymene greater than 1:2, consistent with formation of species of the formulas $[(\text{cymene})(\text{CD}_3\text{CN})_6\text{Ru}_3\text{S}_2]^{2+}$ and possibly $[(\text{CD}_3\text{CN})_9\text{Ru}_3\text{S}_2]^{2+}$. Compound [**6**]$(\text{PF}_6)_2$ was detected in these solutions by ESI-MS and ^{1}H NMR spectroscopy. Attempts to isolate the postulated $[(\text{cymene})_{3-x}(\text{CD}_3\text{CN})_{3x}\text{Ru}_3\text{S}_2]^{2+}$ compounds ($x = 2, 3$) were unsuccessful, including the use of PPh_3 or 9S3 as trapping ligands. Compounds [**3**]$(\text{PF}_6)_2$ and [**4**]$(\text{PF}_6)_2$ proved relatively unreactive toward photolysis, whereas photolysis of [**5**]$(\text{PF}_6)_2$ in CD_3CN resulted in the slow formation of free cymene.

$[(\text{cymene})_4\text{Ru}_5\text{S}_4](\text{PF}_6)_2$. Extensive handling or photolysis of [**2**]$(\text{PF}_6)_2$ for more than 4 h resulted in decomposition, and two of the decomposition products were characterized crystallographically. The first is $[(\text{cymene})_4\text{Ru}_5\text{S}_4](\text{PF}_6)_2$ ([**6**]$(\text{PF}_6)_2$), which is formed in up to 15% yield during the prolonged irradiation experiments as measured by ^{1}H NMR spectroscopy. Crystallographic analysis confirmed that the dication in [**6**]$(\text{PF}_6)_2$ consists of a Ru_5S_4 core (Figure 4, Table 4). The Ru atoms form a “bow-tie” structure with two trigonal bipyramids sharing a common Ru vertex. The Ru_3 planes are related by an angle of 54.8°. Four Ru atoms are bound to η^6-cymene ligands, while the fifth Ru atom is situated at the knot of the bow tie, bound to four S and four Ru atoms. The average Ru−Ru distance in **6** (2.755 Å) is shorter than the averages for [**1**]$(\text{PF}_6)_2$, [**3**]$(\text{PF}_6)_2$, [**4**]$(\text{PF}_6)_2$, and [**5**]$(\text{PF}_6)_2$ (Figure 5). However, the average Ru−S distance of 2.279 Å is longer than that for [**1**]$(\text{PF}_6)_2$, [**3**]$(\text{PF}_6)_2$, [**4**]$(\text{PF}_6)_2$, or [**5**]$(\text{PF}_6)_2$ but is still within the range for Ru−S single bonds for μ_3-S−Ru_3 complexes.

After isolation of [**6**]$(\text{PF}_6)_2$, the remaining solution was treated with excess PPh_3 to generate crystals of $[\text{Ru}(\text{PPh}_3)_2(\text{CH}_3\text{CN})_4](\text{PF}_6)_2$ ([**7**]$(\text{PF}_6)_2$), which were identified by single-crystal X-ray diffraction and is not further described here. This finding demonstrates that $\text{Ru}(\text{CH}_3\text{CN})_6^{2+}$ may be formed as either a thermal or photolytic product in the decomposition of $[(\text{cymene})_2(\text{CH}_3\text{CN})_3\text{Ru}_3\text{S}_2](\text{PF}_6)_2$.

Electrochemistry Cyclic voltammetry established that, like [**1**]$(\text{PF}_6)_2$, compounds [**3**]$(\text{PF}_6)_2$, [**4**]$(\text{PF}_6)_2$, and [**5**]$(\text{PF}_6)_2$ are all electroactive. These results are summarized in Table 5. For comparison, the cyclic voltammogram of [**1**]$(\text{PF}_6)_2$ was obtained using the same experimental conditions and was found to have two very closely spaced reductions at −1.09 and −1.21 V. Compound [**3**]$(\text{PF}_6)_2$ underwent two closely spaced reductions, at −1.21 and −1.36 V relative to $\text{Fc}^{+/0}$. Compound [**4**]$(\text{PF}_6)_2$ underwent two quasireversible reductions, centered at −1.10 and −1.25 V. Because the CV patterns for [**3**]$(\text{PF}_6)_2$ and [**4**]$(\text{PF}_6)_2$ so closely resemble that of **1**, these reductions are assumed to each consist of a pair of one-electron reductions. The reductions are reversible based on peak separation ($i_{\text{pa}}-i_{\text{pc}}$) and the i_a/i_c ratios vs an internal $\text{Fe}^{+/0}$ standard. Compound [**5**]$(\text{PF}_6)_2$, however, was found to undergo one irreversible reduction centered at −1.37 V and one reversible reduction centered at −2.00 V, also relative to ferrocene. No oxidative activity was observed in any of these compounds.

Discussion

It is known that Ru(II)−arene compounds are susceptible to photolysis in acetonitrile to give the corresponding $\text{LRu}(\text{CH}_3\text{CN})_3^{n+}$ derivatives. The corresponding photolyses of CH_3CN solutions of $[(\text{cymene})_3\text{Ru}_3\text{S}_2]^{2+}$ were therefore expected to give $[(\text{cymene})_2(\text{CH}_3\text{CN})_3\text{Ru}_3\text{S}_2]^{2+}$, and our experiments show that this is the case. It was also established that CH_3CN participates in the labilization process, in agreement with previous studies that have shown the rate-determining step of arene displacement by CH_3CN is the nucleophilic attack on Ru by a solvent molecule.[24] However, we were only able to prepare CH_3CN

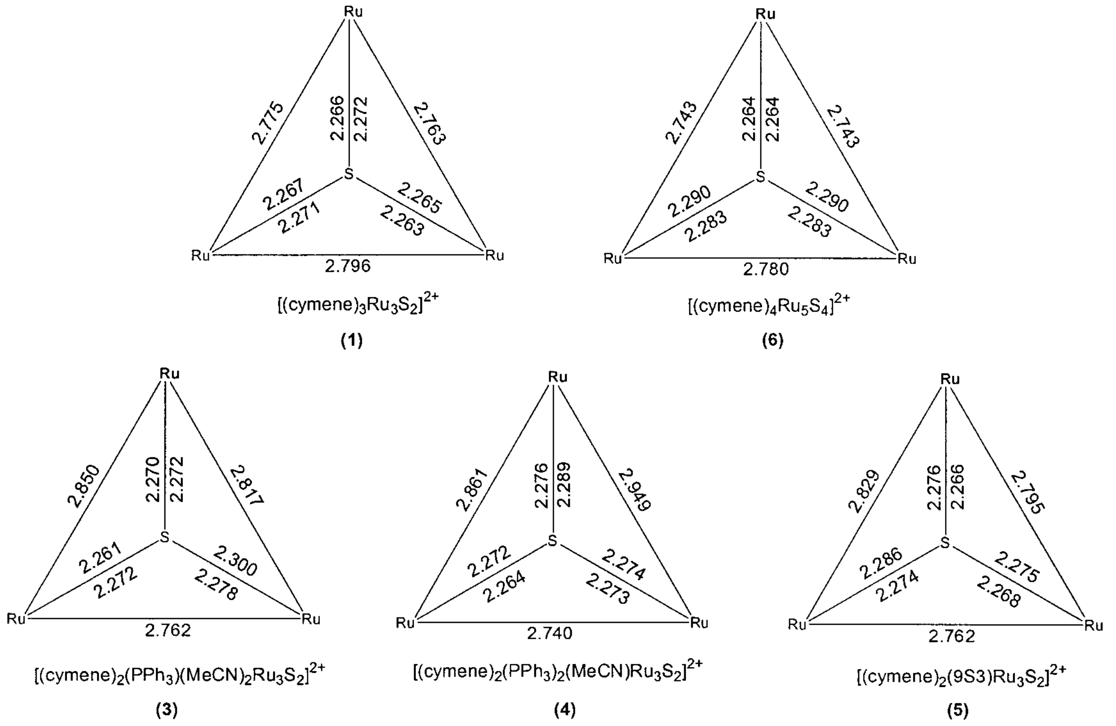

Figure 5. Schematic representations of the Ru_3S_2 cores of **1** and **3**−**6** are shown with the substituted Ru in bold and the pair of μ_3-S atoms eclipsed. In **6**, the Ru_3 "halves" are related by symmetry.

Table 5. Reduction Potentials in Volts (V) for **1** and Its Derivatives with Respect to Fc^+/Fc[a]

C^{2+}	$C^{2+/1+}$	$C^{1+/0}$
$[(cymene)_3Ru_3S_2]^{2+}$	−1.09	−1.21
$[(cymene)_2(PPh_3)(MeCN)_2Ru_3S_2]^{2+}$	−1.21	−1.36
$[(cymene)_2(PPh_3)_2(MeCN)Ru_3S_2]^{2+}$	−1.10	−1.25
$[(cymene)_2(9S3)Ru_3S_2]^{2+}$	−1.37[b]	−2.00

[a] All couples are reversible or quasireversible unless otherwise noted, based on peak separation and $i_a/i_c \approx 1$. Further details are given in the Experimental Section. [b] Irreversible.

derivatives, but not acetone or aqua complexes, although preparation of $[CpRu(acetone)_3]^+$ via photolysis has been reported.[31] A wide variety of Ru(arene) carbonyl clusters have been synthesized,[32] but the photolyses of these clusters have not been explored although it is known that CH_3CN substitution of inert Ru carbonyl clusters gives catalytically active species.[33]

We were able to establish the formation of $[(cymene)_2(CH_3CN)_3Ru_3S_2](PF_6)_2$ by trapping it with PPh_3 to form $[(cymene)_2(CH_3CN)_{3-x}(PPh_3)_xRu_3S_2]^{2+}$, where $x = 1, 2$. The behavior of these compounds closely resembles that of $[CpRu(CH_3CN)_3]^+$ in which one CH_3CN is easily replaced by $P(OR)_3$ to give $[CpRu(CH_3CN)_2(P(OR)_3)]^+$, but a noncoordinating solvent and more extreme conditions are needed to replace the second and third CH_3CN ligands.[19]

The redox activity of compounds [**3**]$(PF_6)_2$ and [**4**]$(PF_6)_2$ closely resembles that of the starting material [**1**]$(PF_6)_2$, with each compound undergoing two closely spaced one-electron reductions at similar potentials. We assume that these reductions involve the breaking of one Ru−Ru bond as the two-electron reduction of [**1**]$(PF_6)_2$, which yields *nido*-$[(cymene)_3Ru_3S_2]^0$ with two Ru−Ru bonds.[17] That the compounds [**3**]$(PF_6)_2$, [**4**]$(PF_6)_2$, and [**5**]$(PF_6)_2$ are electroactive suggests that the reduced forms of these compounds may be chemically generated and isolated. These neutral compounds would be even more electron-rich and thus possibly more reactive toward small molecules. The photolability of the arene ligands in reduced derivatives of [**1**]$(PF_6)_2$ is the subject of continuing studies.

Attempts to isolate the $[(cymene)_2(CH_3CN)_3Ru_3S_2](PF_6)_2$ using traditional recrystallization methods proved unsuccessful; instead we obtained the bow-tie cluster **6**, $[(cymene)_4Ru_5S_4](PF_6)_2$. Several similar compounds have been previously characterized electrochemically.[34−36] Cluster **6** may be viewed as a derivative of a $[(cymene)_3Ru_3S_2]$ cluster wherein one cymene ligand has been replaced by a $[(cymene)_2Ru_2S_2]$ "ligand". This view of the cluster suggests a mechanism for its formation:

$$2\underset{\mathbf{2}}{[(\text{cymene})_2(\text{CH}_3\text{CN})\text{Ru}_3\text{S}_2]^{2+}} \rightarrow \underset{\mathbf{6}}{[(\text{cymene})_4\text{Ru}_5\text{S}_4]^{2+}} + [\text{Ru}(\text{CH}_3\text{CN})_6]^{2+} \quad (4)$$

Solvolysis of $[(cymene)_2(CH_3CN)_3Ru_3S_2]^{2+}$ would give $[Ru(CH_3CN)_6]^{2+}$, detected as its PPh_3 adduct **7**, and $[(cymene)_2Ru_2S_2]$, which could then displace CH_3CN from $[(cymene)_2(CH_3CN)_3Ru_3S_2](PF_6)_2$. The ready formation of **6** limits the versatility of **2**.[37]

Experimental Section

Materials. Photolysis employed an immersion reactor (volume = 150 mL) with a nitrogen inlet and a water-cooled quartz sheath. The

---

(31) Schrenk, J. L.; Mann, K. R. *Inorg. Chem.* **1986**, *25*, 1906−1908.

(32) Braga, D.; Dyson, P. J.; Grepioni, F.; Johnson, B. F. G. *Chem. Rev.* **1994**, *94*, 1585−1620.

(33) Foulds, G.; Johnson, B. F. G.; Lewis, J. *J. Organomet. Chem.* **1985**, *296*, 147−153.

(34) Bolinger, C. M.; Weatherill, T. D.; Rauchfuss, T. B.; Rheingold, A. L.; Day, C. S.; Wilson, S. R. *Inorg. Chem.* **1986**, *25*, 634−643.

(35) Tang, Z.; Nomura, Y.; Kuwata, S.; Ishii, Y.; Mizobe, Y.; Hidai, M. *Inorg. Chem.* **1998**, *37*, 4909−4920.

(36) Eremenko, I. L.; Pasynskii, A. A.; Gasanov, G. S.; Orazsakhatov, B.; Struchkov, Y. T.; Shklover, V. E. *J. Organomet. Chem.* **1984**, *275*, 183−189.

(37) Subsequent to submission of this paper, Hidai et al. have described $(cymene)_4Ru_4S_4$: Seino, H.; Mizobe, Y.; Hidai, M. *New J. Chem.* **2000**, *24*, 907−911.

Table 6. Details of Data Collection and Structure Refinement for the $\mathrm{PF_6^-}$ Salts of Compounds **3**, **4**, **5**, and **6**

	[**3**]$(\mathrm{PF_6})_2$	[**4**]$(\mathrm{PF_6})_2$	[**5**]$(\mathrm{PF_6})_2$	[**6**]$(\mathrm{PF_6})_2$
empirical formula	$\mathrm{C_{42}H_{49}F_{12}N_2P_3Ru_3S_2}$	$\mathrm{C_{58}H_{61}F_{12}NP_4Ru_3S_2}$	$\mathrm{C_{26}H_{40}F_{12}P_2Ru_3S_5}$	$\mathrm{C_{40}H_{56}F_{12}P_2Ru_5S_4}$
fw	2622.25	1635.50	1190.96	1460.38
space group	$P\bar{1}$	$P\bar{1}$	$P\bar{1}$	$I4(1)/acd$
temp, K	153(2)	193(2)	193(2)	193(2)
λ, Å	0.710 69	0.710 73	0.710 73	0.710 73
a, Å	19.769(8)	12.178(5)	12.009(3)	19.3601(5)
b, Å	12.458(6)	13.974(5)	12.218(3)	19.3601(5)
c, Å	23.003(9)	21.528(13)	15.025(4)	26.7167(11)
α, deg	89.07(2)	87.97(6)	83.97(3)	90
β, deg	114.33(2)	84.82(6)	80.99(3)	90
γ, deg	95.70(2)	67.23(5)	71.09(3)	90
V, Å^3	5135(4)	3364(3)	2056.3(9)	10013.8(6)
Z	2	2	2	8
ρ_{calcd}, mg/m^3	1.696	1.615	1.923	1.937
μ (Mo Kα), mm^{-1}	1.124	0.900	1.625	1.778
$F(000)$	1176	1656	2616	5744
GOF	1.058	1.021	1.087	1.017
R1 [$I > 2\sigma$] (all data)[a]	0.0669 (0.0952)	0.0581 (0.0784)	0.0326 (0.0369)	0.0253 (0.0425)
wR2 [$I > 2\sigma$] (all data)[b]	0.1687 (0.1946)	0.1503 (0.1736)	0.0893 (0.0917)	0.0576 (0.0618)

[a] $\mathrm{R1} = \sum||F_o| - |F_c||/\sum|F_o|$. [b] $\mathrm{wR2} = \{\sum[w(F_o^2 - F_c^2)^2]/\sum[w(F_o^2)^2]\}^{1/2}$; $w = 1/\{\sigma^2(F_o^2)\}$.

UV light source was either a high-pressure mercury-vapor lamp (25 W) made by Original Hanau or a similar lamp (200 W) made by Hanovia, which was used with a 250 mL reactor. Solvents used, unless otherwise specified, were distilled under nitrogen over drying agents ($\mathrm{CH_3CN}$ over $\mathrm{CaH_2}$, THF over K/benzophenone, and ether over Na/K/benzophenone). Deuterated solvents were used as received. The starting material $[(\mathrm{cymene})_3\mathrm{Ru_3S_2}](\mathrm{PF_6})_2$ (**1**) was prepared as previously described.[17] The ligands $\mathrm{PPh_3}$ and 1,4,7-trithiacyclononane were used as received.

Methods. Elemental analyses were done by the University of Illinois Microanalytical Laboratory. ^{1}H NMR spectra were acquired on a Bruker AC 250, AMX 300, a Unity Varian 400, or a Unity Varian 500 spectrometer. $^{31}\mathrm{P}\{^1\mathrm{H}\}$ NMR spectra were acquired on either a Unity Varian 400 or a Unity Varian 500 spectrometer. All $^{31}\mathrm{P}\{^1\mathrm{H}\}$ spectra were referenced to an external 85% $\mathrm{H_3PO_4}$ standard. Electrochemical experiments were done on a BAS-100 electrochemical analyzer. Cyclic voltammograms were measured at a scan rate of 50 mV/s on 10^{-3} M $\mathrm{CH_3CN}$ solutions using 0.01 M $\mathrm{Bu_4NPF_6}$ as supporting electrolyte and referenced to $\mathrm{Fc^{+/0}}$. A platinum wire counter electrode, a glassy carbon working electrode, and a $\mathrm{Ag/AgPF_6(CH_3CN)}$ reference electrode were used. All operations were carried out using standard Schlenk techniques.

$[(\mathrm{cymene})_2(\mathrm{CD_3CN})_3\mathrm{Ru_3S_2}](\mathrm{PF_6})_2$ ([2-d_9]$(\mathrm{PF_6})_2$). A solution of 5 mg (0.0047 mmol) of **1** in 1 mL of $\mathrm{CD_3CN}$ was irradiated for 6 h during which time the color of the solution darkened from red-brown to dark-brown. The ^{1}H NMR spectra of the reaction solution showed the formation of free cymene and a new set of signals assigned to **2**-$d_9{}^{2+}$. Resonances for **1** disappeared within 1 h. The compound $[(\mathrm{cymene})_2(\mathrm{CH_3CN})_3\mathrm{Ru_3S_2}](\mathrm{PF_6})_2$ ([**2**]$(\mathrm{PF_6})_2$) was prepared similarly. Irradiation of a 10:1 acetone-d_6/$\mathrm{CD_3CN}$ solution of [**1**]$(\mathrm{PF_6})_2$ also gave [**2**-d_9]$(\mathrm{PF_6})_2$, requiring >4 h for the resonances of **1** to disappear. ^{1}H NMR ($\mathrm{CD_3CN}$): δ 5.65 (q, J = 6, 18 Hz, 4H), 2.42 (sept, J = 7 Hz, 1 H), 2.19 (s, 3 H), 1.19 (d, J = 7 Hz, 6 H). ESI-MS: m/z = 339 ($[(\mathrm{cymene})_2(\mathrm{CD_3CN})\mathrm{Ru_3S_2}]^{2+}$), 359 ($[(\mathrm{cymene})_2(\mathrm{CD_3CN})_2\mathrm{Ru_3S_2}]^{2+}$), 823 ($[(\mathrm{cymene})_2(\mathrm{CD_3CN})\mathrm{Ru_3S_2}](\mathrm{PF_6})^{1+}$), and 864 ($[(\mathrm{cymene})_2(\mathrm{CD_3CN})_2\mathrm{Ru_3S_2}](\mathrm{PF_6})^{1+}$).

$[(\mathrm{cymene})_2(\mathrm{CH_3CN})_2(\mathrm{PPh_3})\mathrm{Ru_3S_2}](\mathrm{PF_6})_2$ ([3]$(\mathrm{PF_6})_2$). A solution of [**2**]$(\mathrm{PF_6})_2$ was generated by photolysis of a solution of 0.195 g (0.184 mmol) of $[(\mathrm{cymene})_3\mathrm{Ru_3S_2}](\mathrm{PF_6})_2$ in 75 mL of $\mathrm{CH_3CN}$ for 1.75 h. The dark-brown solution was treated with a solution of $\mathrm{PPh_3}$ (0.65 g, 0.57 mmol) in 5 mL of $\mathrm{CH_3CN}$. The mixture was stirred for 15 min and then was evaporated over the course of 60 min. The brown residue was redissolved in 4 mL of THF. Immediate addition of 25 mL of ether gave dark-brown microcrystals. Yield: 0.142 g (67%). ^{1}H NMR ($\mathrm{CD_3CN}$): δ 5.13 (q, J = 6, 35 Hz, 4H), 2.56 (sept, J = 7 Hz, 1 H), 2.28 (s, 3 H), 1.23 (d, J = 7 Hz, 6 H). $^{31}\mathrm{P}\{^1\mathrm{H}\}$ NMR ($\mathrm{CD_3CN}$): δ 67 (s), −143 (sept). ESI-MS (THF): m/z = 449 ($[(\mathrm{cymene})_2(\mathrm{PPh_3})\mathrm{Ru_3S_2}]^{2+}$), 1084 ($[(\mathrm{cymene})_2(\mathrm{CH_3CN})(\mathrm{PPh_3})\mathrm{Ru_3S_2}](\mathrm{PF_6})^{1+}$), and 1126 ($[(\mathrm{cymene})_2(\mathrm{CH_3CN})_2(\mathrm{PPh_3})\mathrm{Ru_3S_2}](\mathrm{PF_6})^{1+}$). ESI-MS ($\mathrm{CH_3CN}$): m/z = 449 ($[(\mathrm{cymene})_2(\mathrm{PPh_3})\mathrm{Ru_3S_2}]^{2+}$), 470 ($[(\mathrm{cymene})_2(\mathrm{CH_3CN})(\mathrm{PPh_3})\mathrm{Ru_3S_2}]^{2+}$), 1126 ($[(\mathrm{cymene})_2(\mathrm{CH_3CN})_2(\mathrm{PPh_3})\mathrm{Ru_3S_2}](\mathrm{PF_6})^{1+}$). Anal. Calcd for $\mathrm{C_{42}H_{49}F_{12}N_2P_3Ru_3S_2}$: C, 39.72; H, 3.89; N, 2.21. Found: C, 39.32; H, 4.10; N, 2.30.

$[(\mathrm{cymene})_2(\mathrm{CH_3CN})(\mathrm{PPh_3})_2\mathrm{Ru_3S_2}](\mathrm{PF_6})_2$ ([4]$(\mathrm{PF_6})_2$). A solution of [**2**]$(\mathrm{PF_6})_2$ generated from a 1.75 h photolysis of 0.134 g (0.09 mmol) of $[(\mathrm{cymene})_3\mathrm{Ru_3S_2}](\mathrm{PF_6})_2$ in 75 mL of $\mathrm{CH_3CN}$ was evaporated in vacuo. The residue was taken up in 5 mL of acetone, and this solution was treated with 0.33 g (1.25 mmol) of $\mathrm{PPh_3}$. After 40 min the solvent was removed in vacuo. The remaining solid was then dissolved in 10 mL of THF. Addition of 20 mL of ether gave dark-brown microcrystals. Yield: 0.168 g (89%). ^{1}H NMR ($\mathrm{CD_3CN}$): δ 4.84 (q, J = 6 Hz, 4H), 2.71 (sept, J = 7 Hz, 1 H), 2.34 (s, 3 H), 1.32 (d, J = 7 Hz, 6 H). $^{31}\mathrm{P}\{^1\mathrm{H}\}$ NMR ($\mathrm{CD_3CN}$): δ 44 (s), −143 (sept). ESI-MS ($\mathrm{CH_3CN}$): m/z = 580 ($[(\mathrm{cymene})_2(\mathrm{PPh_3})_2\mathrm{Ru_3S_2}]^{2+}$) and 1347 ($[(\mathrm{cymene})_2(\mathrm{CH_3CN})(\mathrm{PPh_3})_2\mathrm{Ru_3S_2}](\mathrm{PF_6})^{1+}$). Anal. Calcd for $\mathrm{C_{58}H_{61}F_{12}N_1P_4Ru_3S_2}$: C, 46.71; H, 4.12; N, 0.94. Found: C, 46.43; H, 4.06; N, 1.26.

$[(\mathrm{cymene})_2(\mathrm{9S3})\mathrm{Ru_3S_2}](\mathrm{PF_6})_2$ ([5]$(\mathrm{PF_6})_2$). A solution of [**2**]$(\mathrm{PF_6})_2$ was generated by photolyzing 0.135 g (0.127 mmol) of [**1**]$(\mathrm{PF_6})_2$ in 50 mL of $\mathrm{CH_3CN}$ for 1.75 h. The solution was transferred to a flask containing 0.046 g (0.25 mmol) of 9S3. The solution was then stirred for 45 min after which time the solvent was removed in vacuo. The brown gummy residue was treated with 7 mL of THF, resulting in a pale-brown solution and a brown powder. The powder was filtered off and recrystallized from 10 mL of $\mathrm{CH_2Cl_2}$ and 10 mL of ether to give brown microcrystals. Yield: 0.065 g (46%). ^{1}H NMR ($\mathrm{CD_3CN}$): δ 5.67 (s, 4H), 2.49 (sept, J = 7 Hz, 1 H), 2.51 (m, 12H), 2.28 (s, 3 H), 1.27 (d, J = 7 Hz, 6 H). ESI-MS ($\mathrm{CH_3CN}$): m/z = 394 ($[(\mathrm{cymene})_2(\mathrm{C_4H_8S_3})\mathrm{Ru_3S_2}]^{2+}$), 408 ($[(\mathrm{cymene})_2(\mathrm{9S3})\mathrm{Ru_3S_2}]^{2+}$), and 962 ($[(\mathrm{cymene})_2(\mathrm{9S3})\mathrm{Ru_3S_2}](\mathrm{PF_6})^{1+}$). Anal. Calcd for $\mathrm{C_{26}H_{40}F_{12}P_2Ru_3S_5}$: C, 28.23; H, 3.65. Found: C, 28.19; H, 4.04.

$[(\mathrm{cymene})_4\mathrm{Ru_5S_4}](\mathrm{PF_6})_2$ ([6]$(\mathrm{PF_6})_2$). A solution of 0.250 g (0.236 mmol) of $[(\mathrm{cymene})_3\mathrm{Ru_3S_2}](\mathrm{PF_6})_2$ in 150 mL of $\mathrm{CH_3CN}$ was photolyzed for 4 h. The volume was then reduced in vacuo to approximately 5 mL. To precipitate, 30 mL of ether was added. A brown-black powder was collected and washed with ether. This product was then redissolved in 2 mL of $\mathrm{CH_3CN}$ and reprecipitated with 20 mL ether, filtered, washed with ether, and dried in vacuo. This product was then extracted with a THF solution containing 3% $\mathrm{CH_3CN}$, yielding a brown solution. This solution was filtered and overlaid with 30 mL of ether to grow crystals of **6**. Yield: ∼0.005 g (2%). ^{1}H NMR ($\mathrm{CD_3CN}$): δ 5.64 (s, 4H), 2.54 (sept, J = 7 Hz, 1 H), 2.23 (s, 3 H), 1.26 (d, J = 7 Hz, 6 H). ESI-MS: m/z = 518 ($[(\mathrm{cymene})_3\mathrm{Ru_5S_4}]^{2+}$), 585 ($[(\mathrm{cymene})_4\mathrm{Ru_5S_4}]^{2+}$), 1315 ($[(\mathrm{cymene})_4\mathrm{Ru_5S_4}](\mathrm{PF_6})^{+}$).

$[\mathrm{Ru}(\mathrm{CH_3CN})_4(\mathrm{PPh_3})_2](\mathrm{PF_6})_2$ ([7]$(\mathrm{PF_6})_2$). A solution of 0.600 g (0.566 mmol) of $[(\mathrm{cymene})_3\mathrm{Ru_3S_2}](\mathrm{PF_6})_2$ in 155 mL of $\mathrm{CH_3CN}$ was prepared in air and irradiated for 3 h. The solvent was removed in vacuo. The residue was redissolved in 3 mL of $\mathrm{CH_3CN}$, and a brown gummy product resulted on addition of 15 mL of ether. The precipitate was washed with ether until it became powdery and was then filtered. This powder was then stirred overnight in 200 mL of CH_3CN and was further followed by recrystallization from 5 mL of CH_3CN and 100 mL of ether to give a brown-black powder. A solution of 50 mg of this product in 10 mL of acetone was treated with 0.13 g (0.49 mmol) of PPh_3. A 3 mL portion of this solution was overlayed with 3 mL of pentane. A brown powder precipitate formed after 1 week. Colorless crystals of **7** grew after 3 months.

Crystallography. The details of crystal data collection and refinement procedures for $[(cymene)_2(CH_3CN)_2(PPh_3)Ru_3S_2](PF_6)_2{\cdot}2\ CH_3CN$ ([**3**]$(PF_6)_2{\cdot}2CH_3CN$), $[(cymene)_2(CH_3CN)(PPh_3)_2Ru_3S_2](PF_6)_2{\cdot}2$ THF ([**4**]$(PF_6)_2{\cdot}2$ THF), $[(cymene)_2(9S3)Ru_3S_2](PF_6)_2{\cdot}CH_2Cl_2$ ([**5**]$(PF_6)_2{\cdot}CH_2Cl_2$), and $[(cymene)_4Ru_5S_4](PF_6)_2$ ([**6**]$(PF_6)_2$) are given in Table 6. Single crystals of [**3**]$(PF_6)_2{\cdot}2CH_3CN$ were grown by overlaying a solution of 0.020 g (0.016 mmol) of [**3**]$(PF_6)_2$ in 1 mL of CH_3CN and 4 mL of THF with 1 mL of pentane and then 4 mL of ether. Crystals of [**4**]$(PF_6)_2{\cdot}2$ THF were grown from a solution of 0.060 g (0.04 mmol) of [**4**]$(PF_6)_2$ in 10 mL of THF overlaid with an equal amount of ether. Crystals of [**5**]$(PF_6)_2{\cdot}CH_2Cl_2$ were grown by overlaying a solution of 0.020 g (0.018 mmol) of [**5**]$(PF_6)_2$ in 4 mL of CH_2Cl_2 with 1 mL of ether. Single crystals were mounted, using perfluoroether oil, to a thin glass fiber. Data were collected at 153(2) K on a Bruker P4 (**6**) and Stoe IPDS (**3**, **4**, **5**) diffractometers. The structures were solved by direct methods, and refinements were done by full-matrix least squares on F^2 for all data with anisotropic thermal parameters for non-hydrogen atoms and istropic parameters for hydrogen atoms. Both PF_6^- moieties in [**3**]$(PF_6)_2{\cdot}2CH_3CN$ and [**4**]$(PF_6)_2{\cdot}2$ THF and one in [**5**]$(PF_6)_2{\cdot}CH_2Cl_2$ were disordered. One THF molecule in [**4**]$(PF_6)_2{\cdot}2THF$ was disordered. The CH_2Cl_2 molecule in [**5**]$(PF_6)_2{\cdot}CH_2Cl_2$ was disordered and the 9S3 ligand was disordered by rotation over two positions. The environments of the two positions were restrained to be chemically equivalent. Disordered moieties were refined as idealized groups with an effective standard deviation of 0.01 Å. Hydrogen atoms were included as riding idealized contributors. The highest peaks in the final difference Fourier map were in the vicinity of Ru atoms for **3**, **4**, and **5** and in the vicinity of F atoms for **6**. An empirical absorption correction was applied to **6** using ψ scans. Final analysis of variance between observed and calaculated structure factors showed no dependence on amplitude or resolution. All calculations were made using the SHELXTL, version 5.101, program package.

Acknowledgment. This research was supported by the National Science Foundation. We thank Professor R. D. Adams for a helpful discussion.

Supporting Information Available: Complete tables of crystallographic data, final atomic coordinates, equivalent isotropic thermal parameters, anisotropic thermal parameters, bond lengths, bond angles, and hydrogen atom coordinates. This material is available free of charge via the Internet at http://pubs.acs.org.

IC0010609